Bulk first-order phase transition in three-flavor lattice QCD with $O(a)$-improved Wilson fermion action at zero temperature

S. Aoki,[1] M. Fukugita,[2] S. Hashimoto,[3] K-I. Ishikawa,[4] N. Ishizuka,[1,5] Y. Iwasaki,[1] K. Kanaya,[1,5] T. Kaneko,[3] Y. Kuramashi,[1,5] M. Okawa,[4] N. Tsutsui,[3] A. Ukawa,[1,5] N. Yamada,[6] and T. Yoshié[1,5]

(JLQCD Collaboration)

[1]*Graduate School of Pure and Applied Sciences, University of Tsukuba, Tsukuba, Ibaraki 305-8571, Japan*
[2]*Institute for Cosmic Ray Research, University of Tokyo, Kashiwa, Chiba 277-8582, Japan*
[3]*High Energy Accelerator Research Organization (KEK), Tsukuba, Ibaraki 305-0801, Japan*
[4]*Department of Physics, Hiroshima University, Higashi-Hiroshima, Hiroshima 739-8526, Japan*
[5]*Center for Computational Science, University of Tsukuba, Tsukuba, Ibaraki 305-8577, Japan*
[6]*RIKEN BNL Research Center, Brookhaven National Laboratory, Upton, New York 11973, USA*

Three-flavor QCD simulation with the $O(a)$-improved Wilson fermion action is made employing an exact fermion algorithm developed for an odd number of quark flavors. For the plaquette gauge action, an unexpected first-order phase transition is found in the strong coupling regime ($\beta \lesssim 5.0$) at relatively heavy quark masses ($m_{PS}/m_V \sim 0.74$–0.87). Strong metastability persists on a large lattice of size $12^3 \times 32$, which indicates that the transition has a bulk nature. The phase gap becomes smaller toward weaker couplings and vanishes at $\beta \simeq 5.0$, which corresponds to a lattice spacing $a \simeq 0.1$ fm. These results imply that realistic simulations of QCD with three flavors of dynamical Wilson-type fermions at lattice spacings in the range $a = 0.1$–0.2 fm are not possible with the plaquette gauge action. Extending the study to improved gauge actions, we do not observe evidence for first-order phase transition, at least within the (β, κ) range we explored. This suggests the possibility that the phase transition either moves away or weakens with improved gauge actions. Possible origins of the phase transition are discussed.

I. INTRODUCTION

Realistic simulations of the strong interaction through lattice QCD require dynamical treatment of up, down, and strange quarks incorporating their pair creation and annihilation effects in the vacuum. While simulations with the dynamical up and down quarks have now become routine (for recent studies, see Refs. [1–4]), adding a dynamical strange quark is still in the development stage. This is primarily because no exact algorithm to treat an odd number of flavors was known until recently. In fact, with the conventional hybrid Monte Carlo (HMC) algorithm [5], the number of flavors is limited to even. The R algorithm [6] can be used for any number of flavors, as applied in recent three-flavor simulations with the staggered quark action [7,8]. However, the results are subject to systematic errors due to a finite step size in the molecular dynamics evolution, and this has to be controlled by taking the limit of zero step size, which is quite computer time consuming.

Recently, however, several exact algorithms for an arbitrary number of flavors have been proposed for both the Wilson-type [9,10] and the staggered-type [11] fermion actions. They have been shown to work with realistic lattice volumes without much increase of computational cost compared to HMC [10,11]. Thus, a practical barrier to performing realistic three-flavor QCD simulations has been eliminated.

The next step toward realistic simulations is to explore the parameter space of the three-flavor lattice QCD to ensure that the system is free from lattice artifacts over a range of lattice spacing a and quark mass m_q adequate for phenomenology. In practice, this means finding a region corresponding to $a \simeq 0.1$–0.2 fm and $m_q = (1/3 \sim 1) \times m_s$, with m_s the physical strange quark mass.

For the Wilson-type fermion action, there is a related important theoretical issue to settle. For an even number of flavors, evidence has been accumulated over the years that vanishing of pion mass at a critical hopping parameter $\kappa_c(\beta)$ ($\beta = 6/g^2$, with g the gauge coupling) is due to spontaneous breaking of flavor-parity rotational symmetry [12,13]. Whether this understanding holds for an odd number of flavors still needs confirmation. It is therefore mandatory to cover the entire parameter space of the lattice action for three-flavor QCD.

In this work, we numerically explore the parameter space (β, κ) of three-flavor lattice QCD with the $O(a)$-improved Wilson fermion action [14]. The three quark flavors are assumed to be degenerate in mass. For the gauge action, we test both the plaquette and renormalization group (RG) improved gauge actions. The $O(a)$-improvement coefficient c_{SW} is fixed to the one-loop perturbative value, as fully nonperturbative values for the relevant gauge actions were not available until after the present work was well in progress [15–17].

For the standard plaquette gauge action, we unexpectedly find [18] a clear evidence of the existence of an ordered phase for large κ separated by a first-order phase transition from the disordered phase at smaller κ. The transition persists for large volumes, and, hence, it is a bulk phase transition. Contrary to the disordered phase, the ordered phase does not exhibit the standard features of the confining phase. For example, the pseudoscalar-to-vector meson mass ratio is similar in the disordered and ordered phases at around 0.8, but the lattice spacing is unnaturally large in the ordered phase. The first-order phase transition is observed in the strong coupling regime. The gap of physical quantities across the transition diminishes toward weaker couplings and appears to vanish at $\beta \simeq 5.0$, which corresponds to a lattice spacing $a \simeq 0.1$ fm.

These results indicate that there is a parameter region which is not smoothly connected to continuum three-flavor QCD. In other words, the continuum three-flavor QCD can be approached only if one uses lattices much finer than $a \simeq 0.1$ fm, if one employs the plaquette gauge action.

We find that the metastability signals disappear if one employs improved gauge actions such as the RG improved action [19] or $O(a^2)$-improved Lüscher-Weisz action [20]. With these actions, the continuum extrapolation should be possible from a conventional range of lattice spacings $a \sim 0.1$–0.2 fm.

The finding of a first-order phase transition for the plaquette gauge action is quite unexpected. A large number of simulations carried out in the past for the quenched and two-flavor cases were consistent with the expectation that the disordered (i.e., confining) phase extends over $0 \leq \kappa \leq \kappa_c$ for any value of β. Recently, however, while making a study of twisted mass QCD, Farchioni *et al.* reported in a two-flavor simulation with unimproved Wilson quark action and plaquette gauge action [21] that there exists a first-order phase transition at $\beta = 5.2$. They suggested that this phase transition can be understood as the alternative to the parity-flavor broken phase which was pointed out by Sharpe and Singleton [22].

It is possible that their finding and ours have a common origin. Another possible explanation for our first-order transition is that it is related to the first-order phase transition encountered in pure $SU(3)$ gauge theory in the extended coupling space (β, β_A), where β_A characterizes the strength of adjoint representation [23–25]. Further work is needed for clarification of the origin of the first-order phase transition for both the two- and three-flavor cases.

The rest of this paper is organized as follows. In Sec. II we introduce the lattice actions and simulation algorithms we employed. Section III describes our study of phase structure of three-flavor lattice QCD with the plaquette gauge action, where the presence of the metastable states is discussed in detail. The phase structure analysis for the case of improved gauge actions is discussed in Sec. IV. In

Sec. V we discuss the possible origin of the first-order transition and related phenomena encountered in past studies. A conclusion is given in Sec. VI where we also discuss the possibility of realistic simulations of three-flavor QCD. The first report of the present work was briefly made in Ref. [18].

II. LATTICE ACTION AND ALGORITHM

The partition function we study is defined by

$$ \mathcal{Z} = \int \mathcal{D}U (\det[D_{ud}])^2 (\det[D_s]) e^{-S_g(U)}. \qquad (1) $$

Here $S_g(U)$ is the gluon action given by

$$ S_g(U) = \frac{\beta}{6} \left[c_0 \sum W_{1\times1} + c_1 \sum W_{1\times2} \right], \qquad (2) $$

where $W_{1\times1}$ and $W_{1\times2}$ are the plaquette and rectangular Wilson loops, respectively. The summations are taken over all possible plaquettes and rectangles on the lattice. The coefficients c_0 and c_1 are determined as $c_0 = 1 - 8c_1$, with $c_1 = 0$, -0.331, or $-1/(12\langle P \rangle^{1/2})$ for the standard Wilson action, the RG-improved action [19], and the $O(a^2)$-improved [Lüscher-Weisz (LW)] action [20], respectively, and $\langle P \rangle$ is the plaquette average introduced for a mean field improvement.

The fermionic determinant $(\det[D_{ud}])^2$ represents the contribution of degenerate up (u) and down (d) quarks, whereas the strange (s) quark effect is given by $(\det[D_s])$. In this work, we consider mainly the $O(a)$-improved Wilson-Dirac operator $D_q = 1 + M_q + T_q$ ($q = u, d, s$), with M_q the usual hopping term including the hopping parameter κ_q and T_q the $O(a)$-improvement Sheikholeslami-Wohlert (SW) term [14]. The explicit form of T_q is given by

$$ T_q = -\tfrac{1}{2} c_{\text{SW}} \kappa_q \sigma_{\mu\nu} \mathcal{F}_{\mu\nu}, \qquad (3) $$

with $\mathcal{F}_{\mu\nu}$ the cloverleaf-type field strength on the lattice. For the coefficient c_{SW} we employ the value determined by tadpole-improved one-loop perturbation theory as

$$ c_{\text{SW}} = \frac{1}{\langle P \rangle^{3/4}} \left(1 + c_{\text{SW}}^{(1)} \frac{6/\beta}{\langle P \rangle} \right), \qquad (4) $$

where $c_{\text{SW}}^{(1)} = 0.0159$ [26–28] for the standard Wilson gauge action. For improved gauge actions it becomes $c_{\text{SW}}^{(1)} = 0.008$ (RG) or 0.013 (LW) [29]. The average plaquette $\langle P \rangle$ is calculated in pure gauge theory with the same value of β.

We employ an exact HMC-type algorithm for three-flavor QCD developed in Ref. [10]. The u and d quark determinant $(\det[D_{ud}])^2$ is estimated by the usual pseudo-fermion integral:

$$ (\det[D_{ud}])^2 = \int \mathcal{D}\phi_{ud}^\dagger \mathcal{D}\phi_{ud} \exp[-|D_{ud}^{-1}\phi_{ud}|^2]. \qquad (5) $$

To represent $(\det[D_s])$ in a similar manner, we approximate the inverse of D_s by the non-Hermitian Chebyshev polynomial [30,31] of order $2n$:

$$1/D_s \approx P_{2n}(D_s) \equiv \sum_{i=0}^{2n} c_i (D_s - 1)^i$$

$$= \prod_{k=1}^{n} (D_s - z_{j(k)}^*)(D_s - z_{j(k)}), \qquad (6)$$

with $z_k = 1 - \exp(i2\pi k/(2n + 1))$ [32] and a reordering index $j(k)$. We then rewrite

$$(\det[D_s]) = \det[D_s P_{2n}(D_s)]$$

$$\times \int \mathcal{D}\phi_s^\dagger \mathcal{D}\phi_s \exp[-|T_n(D_s)\phi_s|^2], \quad (7)$$

with $T_n(D_s) \equiv \sum_{i=0}^{n} d_i (D_s - 1)^i (= \prod_{k=1}^{n}(D_s - z_{j(k)}))$. Introducing a fictitious momentum P conjugate to the link variable U, the effective Hamiltonian for the $2 + 1$-flavor QCD reads

$$H = \tfrac{1}{2}P^2 + S_g(U) + |D_{ud}^{-1}\phi_{ud}|^2 + |T_n(D_s)\phi_s|^2. \quad (8)$$

We take account of the correction factor $\det[D_s P_{2n}(D_s)]$ by the noisy Metropolis test. After a trial configuration U' is accepted by the usual HMC Metropolis test, we make another Metropolis test with the acceptance probability $P_{\text{corr}}[U \to U'] = \min[1, e^{-dS}]$, with $dS = |A(U')^{-1}A(U)\chi|^2 - |\chi|^2$. Here $A = [D_s P_{2n}(D_s)]^{1/2}$ and χ is the Gaussian noise vector with an unit variance. For other details of the algorithm, see Ref. [10].

III. PHASE STRUCTURE FOR THE PLAQUETTE GAUGE ACTION

A. Thermal cycle analysis

We study the phase structure of three-flavor lattice QCD for the plaquette gauge action ($c_1 = 0$) assuming flavor degeneracy $\kappa \equiv \kappa_{ud} = \kappa_s$. Rapid thermal cycles are performed in the (β, κ) parameter space on $4^3 \times 16$ and $8^3 \times 16$ lattices. For a fixed value of β we start a HMC simulation at $\kappa = 0$ and increase κ in units of 0.001 at every 200 HMC trajectories. This process is continued until we reach the point at which we encounter a large violation of HMC energy conservation satisfying $dH > 100$. Then we reverse the process and decrease κ until it reaches the point sufficiently far away from the turning point. This procedure is repeated at a fixed interval over a range of β.

In this global scan, we do not perform the global Metropolis test of HMC or the noisy Metropolis test for the correction factor $\det[D_s P_{2n}(D_s)]$ in Eq. (7). The order of the Chebyshev polynomial is fixed to $2n = 100$ and the molecular dynamics (MD) step size to $d\tau = 1/40$ employing $\tau = 1$ for the length of unit trajectory. The stopping criterion of the BiCGStab solver is such that the residual defined by $|Dx - b|/|b|$ becomes smaller than 10^{-14} (10^{-8}) for Hamiltonian (force) calculation, where D is
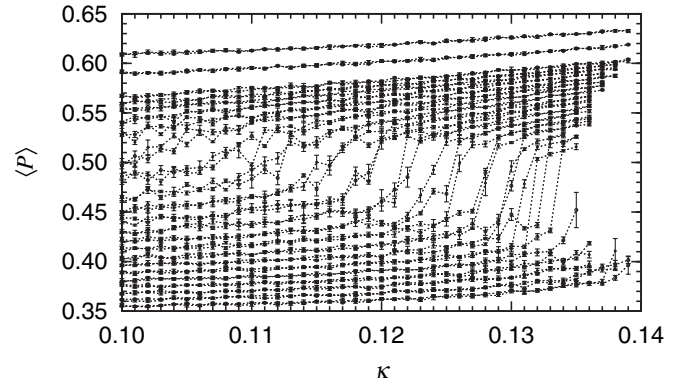

FIG. 1. Thermal cycles of averaged plaquette $\langle P \rangle$ on a $4^3 \times 16$ lattice at $\beta = 4.6$–5.6 with 0.05 steps and 5.8, 6.0 from bottom to top. Each point is measured on 100 trajectories followed by 100 thermalization trajectories from its previous point.

the even-odd preconditioned $O(a)$-improved Wilson-Dirac operator, x is the solution vector, and b is a source vector. The expectation values of observables are measured during the last 100 trajectories after 100 thermalization trajectories at each κ in the cycles.

In Fig. 1 we present the plaquette expectation value $\langle P \rangle$ during thermal cycles on a $4^3 \times 16$ lattice. The value of β increases from $\beta = 4.6$ to 5.6 from bottom to top in units of 0.05. We observe a strong indication of metastability at $4.8 \le \beta \le 5.1$. The system appears to jump from a disordered phase at smaller κ to an ordered phase at larger κ.

On small lattices such as $4^3 \times 16$, the gap and metastability might be attributed to a "finite-temperature phase transition" due to a small spatial size, corresponding to the thermal first-order transition observed for three-flavor QCD with the (unimproved) Wilson fermion action [33]. To examine this possibility, we show $\langle P \rangle$ during the thermal cycles on a spatially larger $8^3 \times 16$ lattice in Fig. 2. While the range of β indicative of metastability is shifted
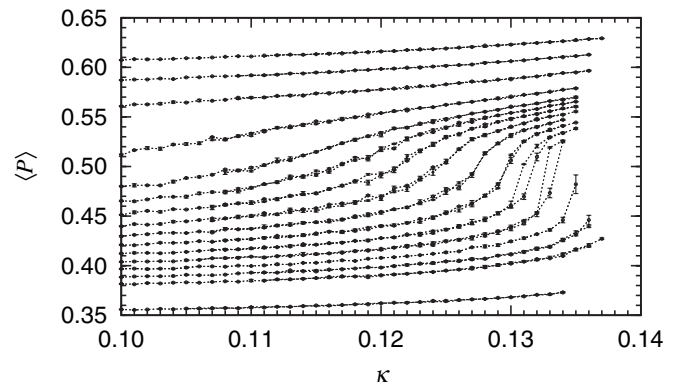

FIG. 2. Thermal cycles of averaged plaquette $\langle P \rangle$ on a $8^3 \times 16$ lattice at $\beta = 4.6$, 4.8–5.3 with 0.05 steps, and 5.4–6.0 with 0.1 steps (from bottom to top) for the standard Wilson gauge action. Each point is measured on 100 trajectories followed by 100 thermalization trajectories from its previous point.
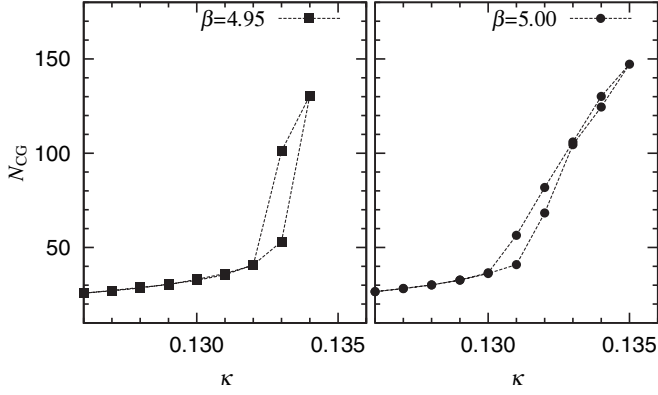
FIG. 3. Number of BiCGStab steps N_{CG} required for the fermion matrix inversion during the HMC trajectories at $\beta = 4.95$ and 5.0 for the standard Wilson gauge action.

and reduced, we still observe a clear hysteresis loop at $\beta = 4.95$ and 5.0.

For the two β values we show the number of BiCGStab iterations N_{CG} required for the fermion matrix inversion

during the calculation of the Hamiltonian (8) with a given stopping criterion 10^{-14} in Fig. 3. We find a large gap in N_{CG} at the point of metastability signals. In the disordered phase N_{CG} is relatively small, whereas in the ordered phase N_{CG} is about a factor $2-3$ larger. As we discuss in the next subsection, the quark mass is heavy at the point of metastability. Indeed, we find $m_{PS}/m_V \simeq 0.83$–0.87. Therefore, the large value of N_{CG}, which implies a small condition number of the Wilson-Dirac operator, in the ordered phase is not attributed to a physically small quark mass.

We suspect the metastability and gap to continue toward strong couplings below $\beta = 4.9$. We cannot confirm it, however, since the thermal cycles encounter a large Hamiltonian difference $dH > 100$ and, hence, are turned back, before finding signals of the ordered phase. For example, at $\beta = 4.8$ this occurs at $\kappa = 0.137$. At this point $N_{CG} = 55.4$, which is still a relatively small number as seen in Fig. 3. The same is true for $\beta = 4.6$ and $\kappa = 0.134$, for which $N_{CG} = 35.6$. Simply reducing the molecular dynamics step size or increasing the polynomial order does not resolve the occurrence of a large value of dH.

TABLE I. Lattice parameters used for the $12^3 \times 32$ simulations. $\langle P_{acc} \rangle$: HMC acceptance rate, N_{MD}: the number of MD steps to proceed a unit trajectory. The molecular dynamics step size is given by $d\tau = 1/N_{MD}$. $\langle P_{corr} \rangle$: global Metropolis test acceptance rate for correction factor, $2n$: the order of the polynomial. The symbols in the "phase" column denote:)L) smaller plaquette value (disordered phase), (H) larger plaquette value (ordered phase), (M) signals are much more unstable and long autocorrelation over 500 trajectories is observed.

β	c_{SW}	κ	$\langle P_{acc} \rangle [N_{MD}]$	$\langle P_{corr} \rangle [2n]$	Phase	am_{PS}	am_V	m_{PS}/m_V	$a_{r_0}^{-1}$ [GeV]
4.88	2.15	0.1345	0.72[50]	0.98[30]	L				
			0.76[64]	0.99[140]	H				
		0.1350	0.91[80]	0.99[42]	L				0.81(7)
			0.81[80]	0.95[300]	H				2.46(7)
4.90	2.14	0.1340	0.70[50]	0.90[24]	L	1.308(7)	1.555(14)	0.84	0.84(1)
			0.71[50]	0.99[100]	H	0.682(14)	0.822(17)	0.83	1.381(3)
		0.1343	0.73[50]	0.86[24]	L	1.247(5)	1.481(21)	0.84	0.83(1)
			0.78[64]	0.98[140]	H	0.458(10)	0.594(21)	0.77	1.90(4)
		0.1345	0.73[50]	0.96[36]	L	1.185(11)	1.405(14)	0.84	0.79(1)
			0.74[64]	0.98[200]	H	0.433(14)	0.587(18)	0.74	1.99(4)
		0.1346	0.85[80]	0.80[120]	H	0.439(14)	0.559(24)	0.78	2.44(7)
4.95	2.11	0.1325	0.76[50]	0.98[30]	L				
		0.1328	0.72[50]	0.97[30]	L	1.285(9)	1.496(16)	0.86	0.827(4)
			0.74[50]	0.99[70]	H	0.844(13)	0.970(16)	0.87	1.39(1)
		0.1330	0.73[50]	0.98[70]	H				
4.97	2.10	0.1320	0.72[50]	0.98[34]	L				
		0.1322	0.77[50]	0.96[30]	L				0.85(1)
		0.1323	0.77[50]	0.99[60]	H				1.35(2)
		0.1325	0.73[50]	0.99[60]	H				
5.00	2.08	0.1310	0.76[50]	0.95[24]	L				
		0.1313	0.75[50]	0.89[26]	L				
		0.1314			M				
		0.1315			M				
		0.1320	0.85[64]	0.99[60]	H				1.53(2)
		0.1330	0.90[100]	0.99[100]	H	0.583(5)	0.692(6)	0.84	2.06(6)
		0.1338	0.90[80]	0.93[100]	H	0.475(10)	0.569(9)	0.83	2.58(4)

Further studies are needed to understand the possible continuation of the ordered phase toward strong couplings.

B. Exact simulation on a larger lattice

To establish the nature of the hysteresis observed in Fig. 2, we perform exact simulations starting from both ordered and disordered configuration with fixed values of β and κ on a $12^3 \times 32$ lattice. The ordered configurations are made at a larger κ value, and the disordered configurations are generated in the quenched limit $\kappa = 0$ at the same β value.

Simulation parameters, including β, c_{SW}, κ, the number of molecular dynamics steps N_{MD}, and the order of the polynomial $2n$, are summarized in Table I. We remark that a polynomial order of only $2n \sim 30$–200 is necessary in order to achieve a $\sim 90\%$ acceptance rate $\langle P_{corr} \rangle$ for the noisy Metropolis test.

Figure 4 shows a representative result which demonstrates clear two-state signals persisting over 1000 trajectories. We confirm that the hysteresis seen in rapid thermal cycles are not an artifact of our inexact simulations in which the HMC and global Metropolis tests are skipped. Similar two-state signals are observed using the R algorithm on a $8^3 \times 16$ lattice. Our observation strongly suggests the existence of a first-order phase transition separating the ordered and disordered phases.

In Table I we list results for pseudoscalar meson mass m_{PS} and vector meson mass m_V in lattice units. We have also calculated the Sommer scale r_0 using the condition $r_0^2 dV(r)/dr|_{r=r_0} = 1.65$ on the static potential. The lattice spacing estimated from the phenomenological value $r_0 = 0.49$ fm is listed in Table I.

In Fig. 5 we plot $(am_{PS})^2$ and am_V at $\beta = 4.9$ as functions of $1/\kappa$. If we extrapolate the data in the disordered phase (solid symbols) linearly as is conventionally made, we find $\kappa_c = 0.13703(29)$ and $m_V(\kappa_c) = 0.67(11)$, which translates into $a_{m_\rho}^{-1} = 0.87(14)$ GeV as a rough es-
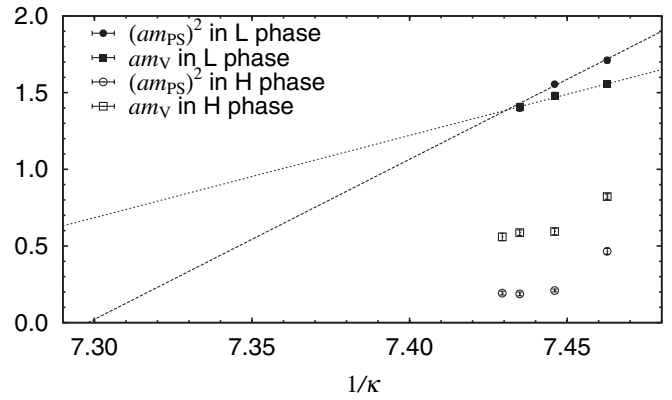
FIG. 5.   Chiral extrapolation of $(am_{PS})^2$ and am_V at $\beta = 4.9$ on a $12^3 \times 32$ lattice. In "H" phase we observe larger plaquette values (ordered phase), and in "L" phase smaller plaquette values are observed (disordered phase).

timate of lattice spacing. These are quite natural values comparable to those encountered in quenched and two-flavor simulations. However, before reaching this point, the three-flavor system makes a transition into an ordered phase in which hadron masses are drastically reduced.

If one looks at the lattice spacing determined from r_0 in Table I, we see that $a_{r_0}^{-1} \approx 0.8$ GeV in the disordered phase, which is consistent with the spectrum estimate from m_ρ above, while $a_{r_0}^{-1} \approx 2$ GeV in the ordered phase is much larger. Furthermore, pion mass squared does not seem to decrease in the ordered phase. We then suspect that physical results cannot be obtained with simulations in the ordered phase.

C. Phase diagram

In Fig. 6 we plot the location of the observed phase transition $\kappa_X(\beta)$ in the (β, κ) plane for various lattice sizes. Open squares for a $4^3 \times 16$ lattice and open circles for a $8^3 \times 16$ lattice show the point of hysteresis observed with the inexact algorithm, while solid circles and open up triangles correspond to the point where two-state signals such as in Fig. 4 are observed with the exact algorithm.

The location of the phase transition line significantly moves when we increase the lattice size from $4^3 \times 16$ to $8^3 \times 16$. However, it stays at the same place when the lattice size is further increased to $12^3 \times 32$, which strongly suggests that the first-order transition line persists in the infinite volume limit at zero temperature. In fact, the gap in the value of $\langle P \rangle$ does not significantly change from $8^3 \times 16$ to $12^3 \times 32$, as shown in Fig. 7.

Figure 7 also shows that the gap in the plaquette expectation value decreases toward larger β and vanishes around $\beta = 5.0$. Since we observe no sign of second-order transition at weaker couplings (Fig. 2), the transition appears to terminate at $\beta \simeq 5.0$.

Toward the strong coupling regime, we expect the phase transition line to continue below the last point of κ_X at $\beta =$
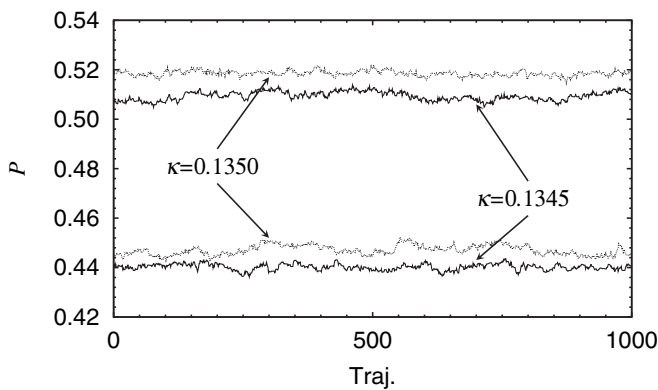

FIG. 4.   A typical example of the two-state signal on a $12^3 \times 32$ lattice at $\beta = 4.88$ and $c_{SW} = 2.15$. The plaquette history is shown. 500–1000 trajectories are devoted to the thermalization from ordered/disordered configurations.

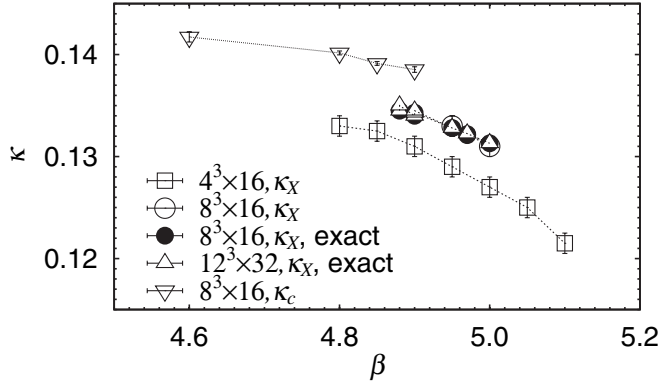FIG. 6. Phase diagram in the (β, κ) plane. Data for the phase transition points κ_X are from the rapid thermal cycles on $4^3 \times 16$ (open squares) and $8^3 \times 16$ (open circles) lattices. Solid circles and open up triangles are from the exact simulation on $8^3 \times 16$ and $12^3 \times 32$ lattices, respectively. The critical hopping parameter κ_c (open down triangles) is estimated using an extrapolation from smaller κ values.

4.88 in Fig. 6. Indications are that the gap tends to become large toward lower β values (see Fig. 7), while the pseudoscalar-to-vector meson mass ratio on the gap is almost independent of β.

The critical hopping parameter κ_c drawn by downward triangles in Fig. 6 represents a rough estimate based on the number of iterations of the BiCGStab solver, N_{CG}, in the calculation of Hamiltonian [Eq. (8)] on a $8^3 \times 16$ lattice. N_{CG} is sampled during the thermal cycles and the estimates are obtained by linearly extrapolating $1/N_{CG}^2$ as a function of $1/\kappa$. As mentioned earlier, the thermal cycles do not extend far toward large values of κ at the β values below 4.88. Therefore, the estimate of κ_c may have a large uncertainty. We also emphasize whether there actually exists the critical κ_c where the pion mass vanishes in the ordered phase is an open issue. In fact, the pion mass measured in the ordered phase at $\beta = 4.9$ shown in Fig. 5 is almost constant as a function of κ.
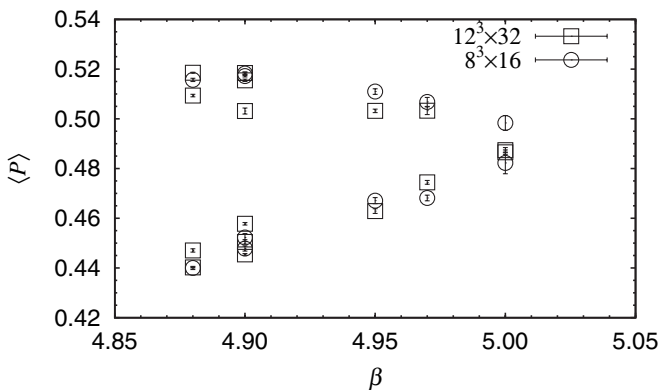

FIG. 7. Plaquette expectation values in the two phases on the first-order phase transition line. Data from the $8^3 \times 16$ and $12^3 \times 32$ lattices are plotted as a function of β.

D. Practical implications

Our findings expose a serious practical problem on simulations using the $O(a)$-improved Wilson fermion action in combination with the plaquette gauge action. To guarantee a smooth extrapolation to the continuum limit, we should carry out simulations at coupling weaker than the termination point of the first-order transition at $\beta \approx 5.0$. As shown in Table I, the lattice spacing estimated from $r_0 = 0.49$ fm at $\beta = 5.0$ is $1/a = 1.53(2)$ GeV ($\kappa = 0.1320$), 2.06(6) GeV ($\kappa = 0.1330$), and 2.58(4) GeV ($\kappa = 0.1338$). The largest κ value ($\kappa = 0.1338$) still corresponds to a heavy quark ($m_{PS}/m_V \sim 0.83$). Taking the significant κ dependence of $1/a$ into account, the lattice spacing in the chiral limit would be even larger, possibly greater than 3 GeV. A 2 fm lattice would then require a $30^3 \times 60$ volume or larger. Large-scale simulations starting at such fine lattices and large lattice volumes are too computer time consuming even with high-end supercomputers available at present. There is another possibility that the pseudoscalar meson mass does not vanish at any κ as described in Ref. [22]. This possibility will be discussed in Sec. V. In this case the realistic simulations are not possible at these lattice parameters.

IV. PHASE STRUCTURE FOR IMPROVED GAUGE ACTIONS

If the first-order transition observed for the plaquette gauge action is a lattice artifact, one may expect that it can be eliminated by improving the gauge action since scaling toward the continuum limit is much improved and the lattice artifacts are expected to be suppressed for these actions.

Here we test two types of improved gauge actions, both of which are defined with (2): one is the RG-improved action [19] and the other is the $O(a^2)$-improved (LW) action [20]. In the LW case, the tadpole factor $\langle P \rangle$ in c_1 is self-consistently determined at $\kappa = 0$ for each β. The clover term is also determined by tadpole-improved one-loop perturbation theory [Eq. (4)] with $\langle P \rangle$ at $\kappa = 0$. Figure 8 shows the results of the thermal cycles on a $8^3 \times 16$ lattice. The simulation conditions, such as the values for $2n$ and $d\tau$ and skipping of the HMC and global Metropolis tests, etc., are the same as those with the unimproved gauge action. In contrast to the case of the plaquette gauge action, we do not observe any remnant of hysteresis loop.

We recall that these results by themselves do not exclude the possibility of a phase transition at larger κ (smaller quark masses) or stronger couplings not covered in the thermal cycle analysis above. We have, however, already started a three-flavor dynamical simulations with the RG-improved gauge action, treating up and down quarks and strange quarks separately [34,35]. At $\beta = 1.90$ and $c_{SW} = 1.715$ ($a^{-1} \sim 2.0$ GeV), we do not encounter a phase transition down to $M_{PS}/M_V \gtrsim 0.62$ on a $20^3 \times 40$ lattice. This is a significantly better situation compared to that with
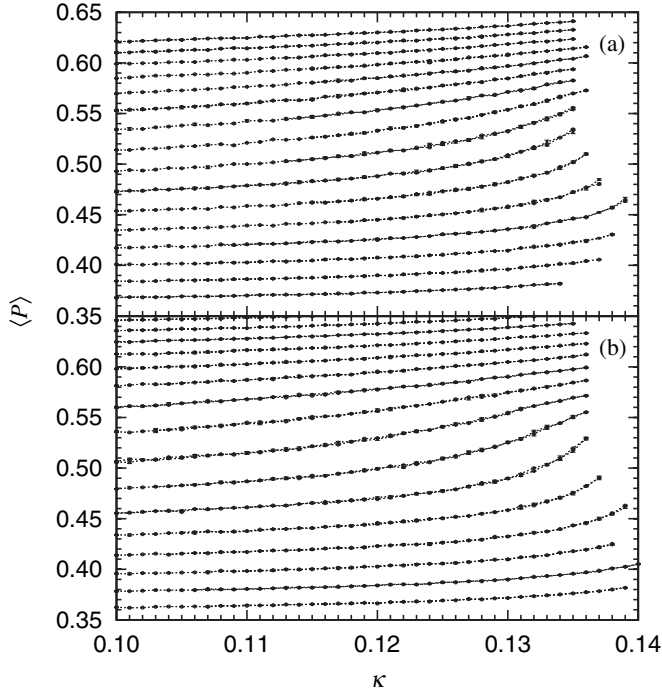
FIG. 8.   Thermal cycles of plaquette expectation value $\langle P \rangle$ on a $8^3 \times 16$ lattice (a) with the RG-improved gauge action at $\beta = 1.50$–2.25 in steps of 0.05 and (b) with tadpole-improved Symanzik gauge action at $\beta = 3.20$–4.70 in steps of 0.10 (from bottom to top).

the plaquette gauge action, for which the phase transition occurs already at a very heavy quark mass of $M_{PS}/M_V \sim 0.83$ at $a^{-1} \sim 1.5$–2.6 GeV or $\beta \sim 5.0$. Thus, improved gauge actions either weaken the phase transition or move it away from the physically relevant region of (κ, β).

V. POSSIBLE ORIGIN OF THE FIRST-ORDER TRANSITION

A. Bulk phase transition in the fundamental-adjoint coupling plane

In the pure SU(3) lattice gauge theory having both fundamental and adjoint couplings β and β_A, a bulk first-order phase transition exists in the strong coupling regime [23–25]. The transition line starts at the purely adjoint point $(\beta, \beta_A) = (0, 6.5(3))$ and extends toward larger β with decreasing β_A. It terminates at (4.00(7), 2.06(8)) and never crosses the purely fundamental line $\beta_A = 0$, so that the pure gauge lattice theory with the fundamental representation is smoothly connected to the continuum limit $\beta = \infty$. Near the critical end point, the correlation function of the 0^{++} glueball channel diverges, but the scaling of other observables is not much affected [25].

This phase transition shares many properties with the one we found in three-flavor lattice QCD. The first-order

transition separates ordered and disordered phases (large and small plaquette expectation values, respectively), and their lattice spacing measured through the string tension is largely different. Furthermore, the transition has a bulk nature; i.e., it remains in the infinite volume limit.

One may suspect that dynamical Wilson fermions effectively induce the adjoint gauge coupling, which gives rise to the bulk transition. This possibility was explored for two-flavor unimproved Wilson fermion action in Ref. [36]. They measured the strength of the induced adjoint coupling on the dynamical configurations and found that it is slightly negative, as opposed to the expectation. The clover term might enhance the induced adjoint coupling as it has a 1×1 Wilson loop structure, but it is to be confirmed either analytically or numerically.

B. Breakdown of parity-flavor symmetry

For two-flavor lattice QCD with the Wilson-type quark action, Sharpe and Singleton [22] carried out an analysis of parity-flavor symmetry using chiral Lagrangian techniques. They pointed out that, depending on the sign of an $O(a^2)$ term, there may be a line of first-order phase transition along which pion mass is nonzero and the chiral condensate flips sign, rather than a pair of second-order transition lines along which pion mass vanishes and parity-flavor symmetry breaks down.

It is straightforward but complicated to extend this type of analysis to the three-flavor case. Since there are three $O(a^2)$ terms allowed in the chiral Lagrangian, rather than a single term for the two-flavor case, predictions are less definite. Nonetheless, one may similarly expect that first-order transitions may occur depending on the coupling of the three terms.

Singular phenomena have been observed with dynamical Wilson-type fermion simulations in a variety of contexts, and our finding is one more of the list of such phenomena. While it is not clear at present if the above analysis offers an understanding of these phenomena, we attempt to discuss them for orientation of future studies.

1. Two-flavor case

Farchioni *et al.* [21] recently reported a first-order phase transition for the plaquette gauge action and unimproved Wilson quark action at $\beta = 5.2$ and $\kappa \approx 0.1715$. They suggested that this phase transition may be understood within the Sharpe-Singleton analysis. [After the submission of this article, Farchioni *et al.* reported the phenomena with the improved gauge (DBW2) action and found that the metastability becomes weaker than that with the plaquette gauge action [37].]

In an old work on the finite-temperature phase transition of two-flavor QCD with the Wilson fermion action, an unexpected strong first-order transition was found [38]. It was suggested that this is a bulk phase transition, since the Polyakov loop does not jump at the transition point below

$\beta \simeq 5.0$, while the plaquette expectation value shows strong metastability.

It is plausible that the two findings refer to the same bulk first-order phase transition. Numerically, Ref. [38] found a metastability at $\beta = 5.22$ and $\kappa = 0.17$, in a close proximity of that in Ref. [21], and the plaquette values in the two phases reported by the two studies are in agreement.

It is not clear if such a first-order phase transition persists when the Wilson quark action is improved by the addition of the clover term. For nonperturbatively $O(a)$-improved Wilson fermion action [39], most physical observables, such as hadron masses and matrix elements, measured in the past simulations [4,40] do not show singular behavior. On the other hand, the mass of 0^{++} glueball is surprisingly lower than in the quenched case [41], perhaps hinting at the presence of a nearby singularity in the coupling constant space. Also, the lattice artifact in the measurement of the light quark mass through the axial-Ward-Takahashi identity is found to be rather large [42].

We also note that the strong first-order transition for the unimproved Wilson quark action disappears if the gauge action is improved [43,44].

2. Three-flavor case

The report by Farchioni *et al.* of a first-order phase transition for the unimproved Wilson quark action and the plaquette gauge action raises the possibility that a similar first-order transition may be present for the three-flavor case. Indeed, in previous finite-temperature studies, a large lattice artifact was found for this action combination [33]: At the point of finite-temperature transition, the light quark mass measured from the axial-Ward-Takahashi identity jumps for $\beta \lesssim 5$, contrary to the expectation that the Ward-Takahashi identity holds at any physical phases with an identical value for the measured quark mass for the same bare parameters.

We have attempted an initial thermal cycle study on $4^3 \times 16$ and $8^3 \times 16$ lattices with unimproved Wilson quark action, and the results are shown in Fig. 9 for the β values in the range 4.6–6.0. We observe a signature of phase transition on the $4^3 \times 16$ lattice (top) at $\beta = 5.1$–5.2, while metastabilities are not apparent on the $8^3 \times 16$ lattice (bottom).

The absence of the gap on the $8^3 \times 16$ lattice does not necessarily mean that the chiral and continuum limit can be smoothly reached, since the thermal cycle above does not cover the small quark mass region. In order to cover this region, we carry out a dedicated run at $\beta = 5.0$. Figure 10 shows the history of plaquette over the HMC trajectories starting from $\kappa = 0.1710$, where the thermal cycle ended, up to 0.1718. We observe large fluctuations of plaquette at $\kappa = 0.1716$ and 0.1718, which may be hinting at the possible presence of a phase transition.

Clearly, further work is needed to reach a comprehensive understanding of the phase structure of lattice QCD
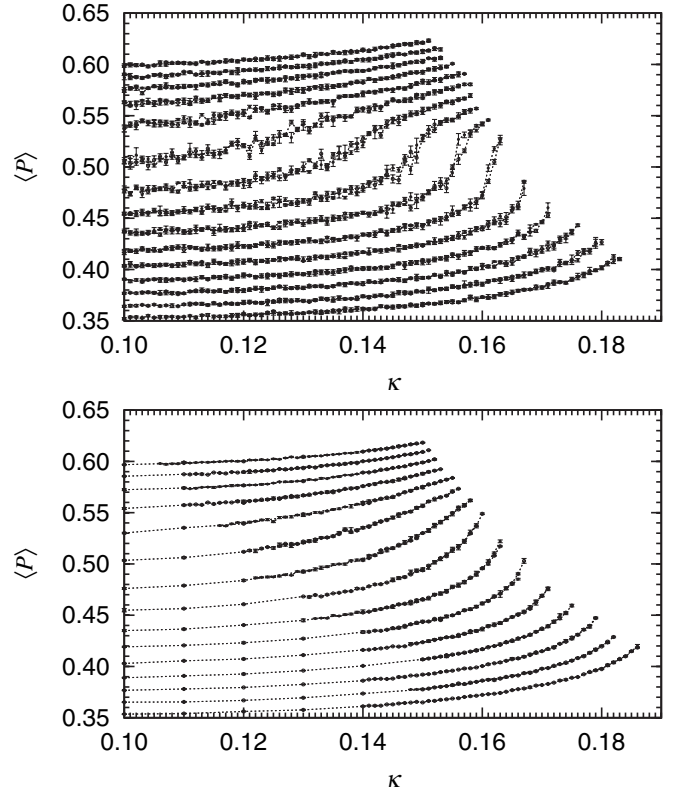

FIG. 9.   Thermal cycles of the plaquette expectation value $\langle P \rangle$ for the plaquette gauge action and unimproved Wilson fermion on $4^3 \times 16$ (top) and on $8^3 \times 16$ (bottom) lattices. The β values in the region 4.6–6.0 are scanned. Lines show different β values in steps of 0.1 (from bottom to top).
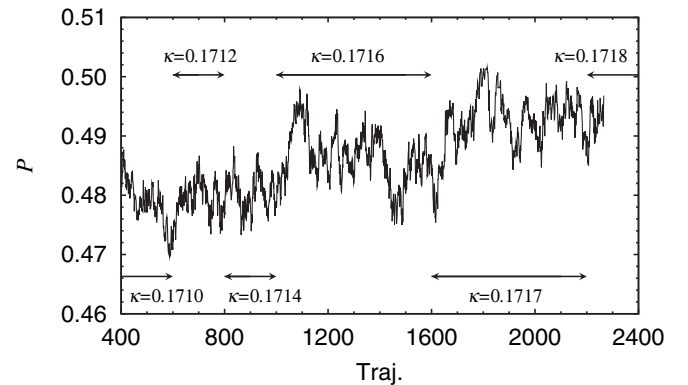

FIG. 10.   Plaquette history of the $N_f = 3$ exact simulation with the plaquette gauge action and the unimproved Wilson fermion action at $\beta = 5.0$. The hopping parameter κ is changed from 0.1710 to 0.1718 as indicated in the plot.

with Wilson-type fermion action for two- and three-flavor cases.

VI. CONCLUSIONS

We have reported the existence of an unexpected phase transition in three-flavor lattice QCD with the

$O(a)$-improved Wilson fermion action. It appears in the strong coupling regime $\beta \lesssim 5.0$ if one uses the standard Wilson plaquette gauge action, while there is no indication of such a phase transition for improved gauge actions. The phase transition persists for large lattice volumes and is likely a bulk phase transition.

Our findings pose a serious practical problem on simulations using the $O(a)$-improved Wilson fermion action in combination with the plaquette gauge action. To avoid unphysical effects of the bulk transition, one has to carry out simulations at couplings weaker than its end point, but the lattice spacing is already smaller than $a \sim 0.1$ fm there, necessitating large lattice volumes and, hence, large computing resources.

This circumstance motivates us to employ the RG-improved gauge action for large-scale three-flavor simulations. A nonperturbative determination of the improvement coefficient c_{SW} for a full $O(a)$ improvement has been made using the Schrödinger functional method [15–17], and preliminary results on the light hadron spectrum have al-ready been presented in Refs. [34,35]. The phase transition is not found at $a^{-1} \sim 2.0$ GeV with $M_{\mathrm{PS}}/M_{\mathrm{V}} \gtrsim 0.62$.

Finally, the recent report that the two-flavor system with the unimproved Wilson action also has a first-order transition and that it may be understood with the context of the Sharpe-Singleton analysis on realizations of the parity-flavor broken phase raises an interesting problem that we need to clarify for phenomenological applications of full QCD simulations with Wilson-type quark actions.

ACKNOWLEDGMENTS

[1] N. Eicker *et al.* (TXL Collaboration), Phys. Rev. D **59**, 014509 (1999).
[2] C. R. Allton *et al.* (UKQCD Collaboration), Phys. Rev. D **60**, 034507 (1999).
[3] A. Ali Khan *et al.* (CP-PACS Collaboration), Phys. Rev. D **65**, 054505 (2002); **67**, 059901(E) (2003).
[4] S. Aoki *et al.* (JLQCD Collaboration), Phys. Rev. D **68**, 054502 (2003).
[5] S. Duane, A. D. Kennedy, B. J. Pendleton, and D. Roweth, Phys. Lett. B **195**, 216 (1987).
[6] S. Gottlieb, W. Liu, D. Toussaint, R. L. Renken, and R. L. Sugar, Phys. Rev. D **35**, 2531 (1987).
[7] C. W. Bernard *et al.*, Phys. Rev. D **64**, 054506 (2001).
[8] C. T. H. Davies *et al.* (HPQCD Collaboration), Phys. Rev. Lett. **92**, 022001 (2004).
[9] T. Takaishi and P. de Forcrand, Int. J. Mod. Phys. C **13**, 343 (2002).
[10] S. Aoki *et al.* (JLQCD Collaboration), Phys. Rev. D **65**, 094507 (2002).
[11] S. Aoki *et al.* (JLQCD Collaboration), Comput. Phys. Commun. **155**, 183 (2003).
[12] S. Aoki, Phys. Rev. D **30**, 2653 (1984); **33**, 2399 (1986); **34**, 3170 (1986); Phys. Rev. Lett. **57**, 3136 (1986).
[13] S. Aoki, A. Ukawa, and T. Umemura, Phys. Rev. Lett. **76**, 873 (1996); Nucl. Phys. B Proc. Suppl. **47**, 511 (1996); S. Aoki, T. Kaneda, A. Ukawa, and T. Umemura, Nucl. Phys. B Proc. Suppl. **53**, 438 (1997).
[14] B. Sheikholeslami and R. Wohlert, Nucl. Phys. **B259**, 572 (1985).
[15] S. Aoki *et al.* (CP-PACS and JLQCD Collaborations), Nucl. Phys. B Proc. Suppl. **119**, 433 (2003).
[16] K-I. Ishikawa *et al.* (CP-PACS and JLQCD Collaborations), Nucl. Phys. B Proc. Suppl. **129**, 444 (2004).
[17] N. Yamada *et al.* (CP-PACS and JLQCD Collaborations), Phys. Rev. D **71**, 054505 (2005); CP-PACS and JLQCD Collaborations (unpublished).
[18] S. Aoki *et al.* (JLQCD Collaboration), Nucl. Phys. B Proc. Suppl. **106**, 263 (2002).
[19] Y. Iwasaki, Report No. UTHEP-118, 1983.
[20] M. Lüscher and P. Weisz, Commun. Math. Phys. **97**, 59 (1985); **98**, 433(E) (1985).
[21] F. Farchioni *et al.*, Eur. Phys. J. C **39**, 421 (2005).
[22] S. R. Sharpe and R. J. Singleton, Phys. Rev. D **58**, 074501 (1998).
[23] J. Greensite and B. Lautrup, Phys. Rev. Lett. **47**, 9 (1981).
[24] G. Bhanot, Phys. Lett. **108B**, 337 (1982).
[25] U. M. Heller, Phys. Lett. B **362**, 123 (1995).
[26] R. Wohlert, DESY Report No. 87/069.
[27] S. Naik, Phys. Lett. B **311**, 230 (1993).
[28] M. Lüscher and P. Weisz, Nucl. Phys. **B479**, 429 (1996).
[29] S. Aoki, R. Frezzotti, and P. Weisz, Nucl. Phys. **B540**, 501 (1999).
[30] A. Boriçi and P. de Forcrand, Nucl. Phys. **B454**, 645 (1995).
[31] A. Borrelli, P. de Forcrand, and A. Galli, Nucl. Phys. **B477**, 809 (1996).
[32] C. Alexandrou, A. Boriçi, A. Feo, P. de Forcrand, A. Galli, F. Jegerlehner, and T. Takaishi, Phys. Rev. D **60**, 034504 (1999).
[33] Y. Iwasaki, K. Kanaya, S. Kaya, S. Sakai, and T. Yoshie, Phys. Rev. D **54**, 7010 (1996).
[34] T. Kaneko *et al.* (CP-PACS and JLQCD Collaborations), Nucl. Phys. B Proc. Suppl. **129**, 188 (2004).
[35] T. Ishikawa *et al.* (CP-PACS and JLQCD Collaborations), Nucl. Phys. B Proc. Suppl. **140**, 225 (2005).

[36] T. Blum, C. DeTar, U. M. Heller, L. Karkkainen, K. Rummukainen, and D. Toussaint, Nucl. Phys. **B442**, 301 (1995).

[37] F. Farchioni *et al.*, Eur. Phys. J. C **42**, 73 (2005).

[38] T. Blum *et al.*, Phys. Rev. D **50**, 3377 (1994).

[39] K. Jansen and R. Sommer (ALPHA Collaboration), Nucl. Phys. **B530**, 185 (1998); **B643**, 517(E) (2002).

[40] C. R. Allton *et al.* (UKQCD Collaboration), Phys. Rev. D **65**, 054502 (2002).

[41] A. Hart and M. Teper (UKQCD Collaboration), Phys. Rev. D **65**, 034502 (2002).

[42] R. Sommer *et al.* (ALPHA Collaboration), Nucl. Phys. B Proc. Suppl. **129**, 405 (2004).

[43] C. W. Bernard *et al.* (MILC Collaboration), Phys. Rev. D **56**, 5584 (1997).

[44] Y. Iwasaki, K. Kanaya, S. Kaya, and T. Yoshie, Phys. Rev. Lett. **78**, 179 (1997).